

Protection of Cystinotic Mice by Kidney-Specific Megalin Ablation Supports an Endocytosis-Based Mechanism for Nephropathic Cystinosis Progression

Virginie Janssens,¹ Héloïse P. Gaide Chevronnay,¹ Sandrine Marie,² Marie-Françoise Vincent,² Patrick Van Der Smissen,¹ Nathalie Nevo,³ Seppo Vainio,⁴ Rikke Nielsen,⁵ Erik I. Christensen,⁵ François Jouret,⁶ Corinne Antignac,³ Christophe E. Pierreux,¹ and Pierre J. Courtoy¹

Due to the number of contributing authors, the affiliations are listed at the end of this article.

ABSTRACT

Background Deletions or inactivating mutations of the cystinosis gene *CTNS* lead to cystine accumulation and crystals at acidic pH in patients with nephropathic cystinosis, a rare lysosomal storage disease and the main cause of hereditary renal Fanconi syndrome. Early use of oral cysteamine to prevent cystine accumulation slows progression of nephropathic cystinosis but it is a demanding treatment and not a cure. The source of cystine accumulating in kidney proximal tubular cells and cystine's role in disease progression are unknown.

Methods To investigate whether receptor-mediated endocytosis by the megalin/LRP2 pathway of ultrafiltrated, disulfide-rich plasma proteins could be a source of cystine in proximal tubular cells, we used a mouse model of cystinosis in which conditional excision of floxed *megalyn/LRP2* alleles in proximal tubular cells of cystinotic mice was achieved by a Cre-LoxP strategy using *Wnt4-CRE*. We evaluated mice aged 6–9 months for kidney cystine levels and crystals; histopathology, with emphasis on swan-neck lesions and proximal-tubular-cell apoptosis and proliferation (turnover); and proximal-tubular-cell expression of the major apical transporters sodium-phosphate cotransporter 2A (NaPi-IIa) and sodium-glucose cotransporter-2 (SGLT-2).

Results *Wnt4-CRE*-driven *megalyn/LRP2* ablation in cystinotic mice efficiently blocked kidney cystine accumulation, thereby preventing lysosomal deformations and crystal deposition in proximal tubular cells. Swan-neck lesions were largely prevented and proximal-tubular-cell turnover was normalized. Apical expression of the two cotransporters was also preserved.

Conclusions These observations support a key role of the megalin/LRP2 pathway in the progression of nephropathic cystinosis and provide a proof of concept for the pathway as a therapeutic target.

JASN 30: 2177–2190, 2019. doi: <https://doi.org/10.1681/ASN.2019040371>

In kidney proximal tubular cells (PTCs), recapture of ultrafiltrated albumin and low molecular weight (LMW) proteins is a major pathway leading to lysosomes.^{1,2} Endocytosis efficiency in PTCs relies on the tandem multiligand receptors, megalin/LRP2 (hereafter simply megalin) and cubilin, which are abundantly expressed and undergo extremely fast endocytosis and recycling.^{3–5} In turn, fast vesicular trafficking relies on high expression in segment 1 (S1) of rate-limiting components of the endocytic machinery depending on mammalian target of

Received April 12, 2019. Accepted July 31, 2019.

C.E.P. and P.J.C. contributed equally to this work.

Published online ahead of print. Publication date available at www.jasn.org.

Correspondence: Prof. Christophe E. Pierreux, de Duve Institute and Université Catholique de Louvain, 75 Avenue Hippocrate, PO Box B1.75.05, 1200-Brussels, Brabant, Belgium. Email: christophe.pierreux@uclouvain.be

Copyright © 2019 by the American Society of Nephrology

rapamycin 1 (mTOR1).^{6,7} Albumin, an abundant ligand in PTC lumen shared by both endocytic receptors, is a globular protein stabilized by 17 disulfide bridges and thus a precursor of 17 cystine molecules. Similarly abundant LMW proteins are additional precursors of cystine. Receptor-mediated endocytosis in PTCs is abrogated upon megalin and cubilin knockout (KO).^{8,9} Perinatal death of most full megalin KO mice¹⁰ can be circumvented by kidney-specific *megalín/LRP2* gene excision (*Meg^{ksKO}* mice); one copy of Wnt4-driven Cre recombinase is sufficient to specifically excise the floxed *megalín/LRP2* gene in virtually all PTCs during nephrogenesis.⁹ Reports indicate megalin ablation does not affect overall PTC histology until approximately 9 months, but causes atrophy of the apical endocytic apparatus (much fewer endosomal vacuoles and dense apical tubules) with secondary effects on fluid-phase endocytosis and sodium-phosphate cotransporter 2A (NaPi-IIa) trafficking.^{11,12} Megalin is also the port of entry of nephrotoxic drugs, such as aminoglycosides,¹³ and this megalin pathway can be targeted by inhibitory drugs.¹⁴ Alternatively, apical PTC endocytosis can be acutely blocked by bolus intravenous injection of dibasic amino acids (especially lysine) in human volunteers¹⁵ and by 1-day oral lysine gavage to rats,¹⁶ but long-term inhibition has not yet been reported.

Nephropathic cystinosis, in brief “cystinosis,” is a rare lysosomal storage disease and the main cause of hereditary renal Fanconi syndrome (reviewed in ¹⁶; for perspective, see ¹⁷). Deletion or inactivating mutations of the cystinosis gene (*CTNS*), encoding the only known lysosomal cystine/hydrogen ion symporter, leads to cystine accumulation and characteristic crystals at acidic pH.¹⁷ Cystine is an obligatory end-degradation product of disulfide-rich proteins,¹⁸ and its accumulation in cystinotic fibroblasts is proportional to the absolute endocytic velocity and relative disulfide abundance in endocytic cargo.^{19,20} Cultured cells also internalize amino acids, and thus cystine, by fluid-phase endocytosis.²¹ The source of lysosomal cystine *in vivo* is unknown.²²

Although lysosomal cystine accumulation occurs in all tissues of patients with nephropathic cystinotic, the kidneys and eyes are first affected. The earliest clinical manifestation is usually a renal Fanconi syndrome combining urinary losses of solutes and LMW proteins. In kidneys, cystinosis leads to PTC apical dedifferentiation and flattening/atrophy, starting at the glomerulo-tubular junction (GTJ) and extending longitudinally downstream (swan-neck deformities);²³ interstitial fibrosis; glomerular lesions; and kidney failure.²⁴ Swan-neck lesions are considered an early adaptation to PTC insult and precede glomerulo-tubular disconnection resulting into atubular glomeruli.^{25–27} Very early, diligent implementation of compliant cysteamine (a cystine-depleting agent and currently the only drug approved by the Food and Drug Administration) treatment was reported to preserve kidney, growth, and thyroid function for over a decade;²⁸ but long-term surveys of large cohorts show delayed progression to kidney insufficiency and other failures, and little control

Significance Statement

Nephropathic cystinosis is the result of deletion or inactivating mutations of the gene encoding the lysosomal cystine transporter cystinosis, but the extent to which disease progression depends on cystine accumulation or transport-independent effects of cystinosis is unknown. Cysteamine, the current treatment to prevent cystine accumulation, delays progression to renal failure but does not correct the Fanconi syndrome nor does it provide a cure. The authors demonstrate that suppression of endocytosis in kidney proximal tubular cells of cystinosis-deficient mice by genetic excision of *megalín/Lrp2* largely prevents cystine accumulation and can help preserve kidney structure and proximal tubular cell differentiation. These observations stress the importance of cystine accumulation in disease progression and provide proof of concept for exploring novel strategies aiming at blocking the megalin pathway.

of the Fanconi syndrome, thus calling for novel therapeutic approaches.^{29,30}

Ctns^{-/-} mice on congenic C57BL/6 background closely reproduce the kidney disease,^{26,31,32} except for a mild/incomplete Fanconi syndrome that has been further vanishing in several colonies including ours, probably due to inbreeding. This mouse model nevertheless was instrumental for deciphering pathogenic and adaptation mechanisms. Pathogenic mechanisms are either transport-related or -independent defects²⁴; their respective contribution to nephropathic cystinosis is unknown. Transport-independent defects include alterations of endolysosomal trafficking,³³ of macroautophagic^{34,35} and chaperone-mediated autophagic fluxes,³⁶ of mTOR complex 1 activation,³⁷ as well as propensity to kidney inflammation.³⁸ Several adaptation mechanisms have been evidenced: (1) early apical PTC dedifferentiation offering reduced workload, as shown by repressed expression of endocytic receptors (megalín and cubilin) and apical solute transporters (main symporters for phosphate, NaPi-IIa, and glucose, sodium-glucose cotransporter-2 [SGLT-2]); (2) active luminal crystal exocytic discharge; and (3) increased PTC turnover with crystal disposal by luminal apoptotic shedding and PTC regeneration by proliferation, which provides fresh lysosomes.²⁶

Calculations predict that uptake of disulfide-rich proteins such as albumin could be the major source of lysosomal cystine accumulation in cystinotic PTCs and thus represent a potential therapeutic pathway.^{24,26} We tested this hypothesis by generating a triple transgenic model: *Ctns*^{-/-}; *Wnt4-CRE*; *Meg^{FL/FL}*, referred to hereafter as *Ctns*^{-/-}/*Meg^{ksKO}* or simply “double KO” mice. Data show that megalín ablation (1) blocks cystine accumulation, thereby preventing crystal deposition in cystinotic kidneys; (2) protects PTCs from structural lesions; and (3) normalizes PTC turnover. The apical expression of NaPi-IIa and SGLT-2 is largely preserved in *Ctns*^{-/-}/*Meg^{ksKO}* mice. These observations support a key role of endocytosis in the progression of nephropathic cystinosis and pave the way to medical intervention targeting the megalín pathway.

METHODS

Mice and Genotyping

Congenic C57BL/6J *Ctns*^{-/-} mice and *Wnt4-Cre* mice (C57BL/6) have previously been described.^{31,39} Mice bearing the *megalin* loxP/loxP gene⁴⁰ were initially generated by Dr. T. Willnow. For genotyping, PCR on DNA extracted from tail samples was used to identify mice bearing wild-type (WT), cystinotic, and floxed *megalin* alleles. The *cystinosin* allele was analyzed with pairs of primers centered on exon 10 (Ex10 forward, 5'-CTCCAGATGTTCTCCAGTC-3'; and Ex10 reverse, 5'-AGTCCGAACCTGGTTGGGT-3') and on the cassette (K7 forward, 5'-GCAGGAATTCGATATCAAGC-3'; and K7 reverse, 5'-AAAGTGGAGGTAGGAAAGAGG-3'). The size of the amplicons revealing the WT and the transgenic *Ctns* allele were 260 and 215 bp, respectively. For *megalin* genotyping, a common forward primer (5'-AGGCTCCGACTTCGTAACG-3') was used with two reverse primers to amplify the WT (5'-TGAAAACCACACTGCTCGATCCGGAAC-3') and/or the floxed allele (5'-ACCTTGCCTGAATTCTGGG-3'). The size of the amplicons was approximately 300 bp for the WT allele and approximately 400 bp for the floxed allele. Presence of the *Wnt4-CRE* transgene was assessed using forward and reverse primers (Cre forward, 5'-GCACGTT-CACCGCATCAAC-3'; and Cre reverse, 5'-CGATGCAACGAGTGATGAGGTTTC-3'; product size 332 bp). Experiments were approved by the Ethical Committee of the Medical School of the Université Catholique de Louvain (2016/UCL/MD/006 and 2018/UCL/MD/026). Mice were treated according to the National Institutes of Health Guide for Care and Use of Laboratory Animals, and used with parsimony.

Tissues

After blood collection, mice were exsanguinated with PBS by perfusion *via* the left ventricle under irreversible anesthesia by 2% xylazine and 50 mg/ml ketamine (250 μ l per mouse, intramuscularly). Fresh tissues (left kidney, spleen, and one liver lobe) were immediately collected using vascular clamps to maintain a closed blood circulatory system, and right kidneys were then fixed *in situ* by switching to whole-body perfusion fixation with cold (4°C, nominal) 4% formaldehyde (from heat-depolymerized paraformaldehyde) in 0.1 M phosphate buffer, pH 7.4, for approximately 3 minutes. They were then excised, decapsulated, and weighed. Hemi-sagittal sections were postfixed by immersion in 4% formaldehyde at 4°C under gentle stirring overnight. Samples were paraffin embedded and 7- μ m-thick sections were collected for histology and confocal fluorescence imaging.

Cystine Assays

A quarter of the unfixed left kidney was homogenized into 600 μ l of 5.2 mM *N*-ethylmaleimide (Sigma-Aldrich) in 10 \times diluted PBS and briefly sonicated, then 200 μ l of 12% 5-sulfosalicylic acid (dehydrated; Merck-Millipore)

was added. Samples were vortexed and frozen at -80°C. Cystine assays were carried out by liquid chromatography-tandem mass spectrometry (liquid chromatography-MS/MS) as previously described⁴¹ with modified MS/MS detection⁴² and normalized to kidney protein. Briefly, the extract was microfuged at 13,000 rpm for 10 minutes at 4°C. The residual pellet was resuspended in 1 ml of 0.1 N sodium hydroxide for protein assay by the Lowry method using BSA as standard. Cystine assays were performed on 50 μ l of supernatant, diluted in water if necessary (according to the 0.2–10 μ M cystine calibration). After butylation, final samples were resuspended in 100 μ l water and 15 μ l was injected into liquid chromatography-MS/MS (Quattro micro; Waters).

Visualization of Cystine Crystals

To highlight cystine crystals by polarized light microscopy, a quarter of the perfused-fixed kidneys were instead postfixed by immersion in alcoholic Bouin solution at 4°C overnight, and then paraffin embedded without any passage in aqueous medium. Sections were deparaffinized and mounted with Q Path Coverquick 3000 mounting medium (Labonord). Slides were analyzed by polarized microscopy at high then low light intensity (highlighting crystals) and recorded images were pseudo-colored in green.

Histology, Multiplex (Immuno)Fluorescence, and Morphometry

Sections were stained with hematoxylin and eosin. For (immuno) fluorescence, antigen retrieval was promoted in citrate buffer, pH 6, at 95°C for 20 minutes using a Lab Vision Pretreatment Module (Thermo Scientific). Tissue was permeabilized with PBS/0.3% Triton X-100 for 5 minutes, and then for a further 1 hour with 10% BSA/3% milk to block nonspecific sites. Sections were incubated overnight at 4°C with the following primary reagents in blocking buffer: sheep anti-megalin (1:800; kindly provided by Dr. P. Verroust and Dr. R. Kozyraki, INSERM U968, Paris, France), rat anti-lysosome-associated membrane protein-1 (anti-LAMP-1; 1:100, 1D4B; Hybridoma Bank), rabbit anti-mouse NaPi-IIa (NaPi-IIa carboxy-terminal peptide, 1:1000; a kind gift from Dr. J. Biber and Dr. C. Wagner, Zurich, Switzerland), rabbit anti-human SGLT-2 (1:100, sc-98975; Santa Cruz Biotechnology), mouse anti-Ki-67 (1:250, 556003; BD-Pharmingen), rabbit anti-active caspase-3 (1:200, 9661; Cell Signaling), or biotinylated *Lotus tetragonolobus* lectin (1:100; Vector Laboratories). After washing, sections were further incubated with the appropriate Alexa Fluor secondary antibodies and/or streptavidin (Invitrogen) or Hoechst bisbenzimidazole H 33258 (Sigma-Aldrich) for 1 hour at room temperature in 10% BSA/0.3% Triton X-100, mounted with Faramount Aqueous Mounting Medium (Dako), and imaged on a spinning disk confocal microscope using an EC Plan-NeoFluar 40 \times /1.3 or 100 \times /1.4 oil differential interference contrast objective (Cell Observer Spinning Disk; Zeiss). Differential interference contrast (Nomarski microscopy) images were obtained using

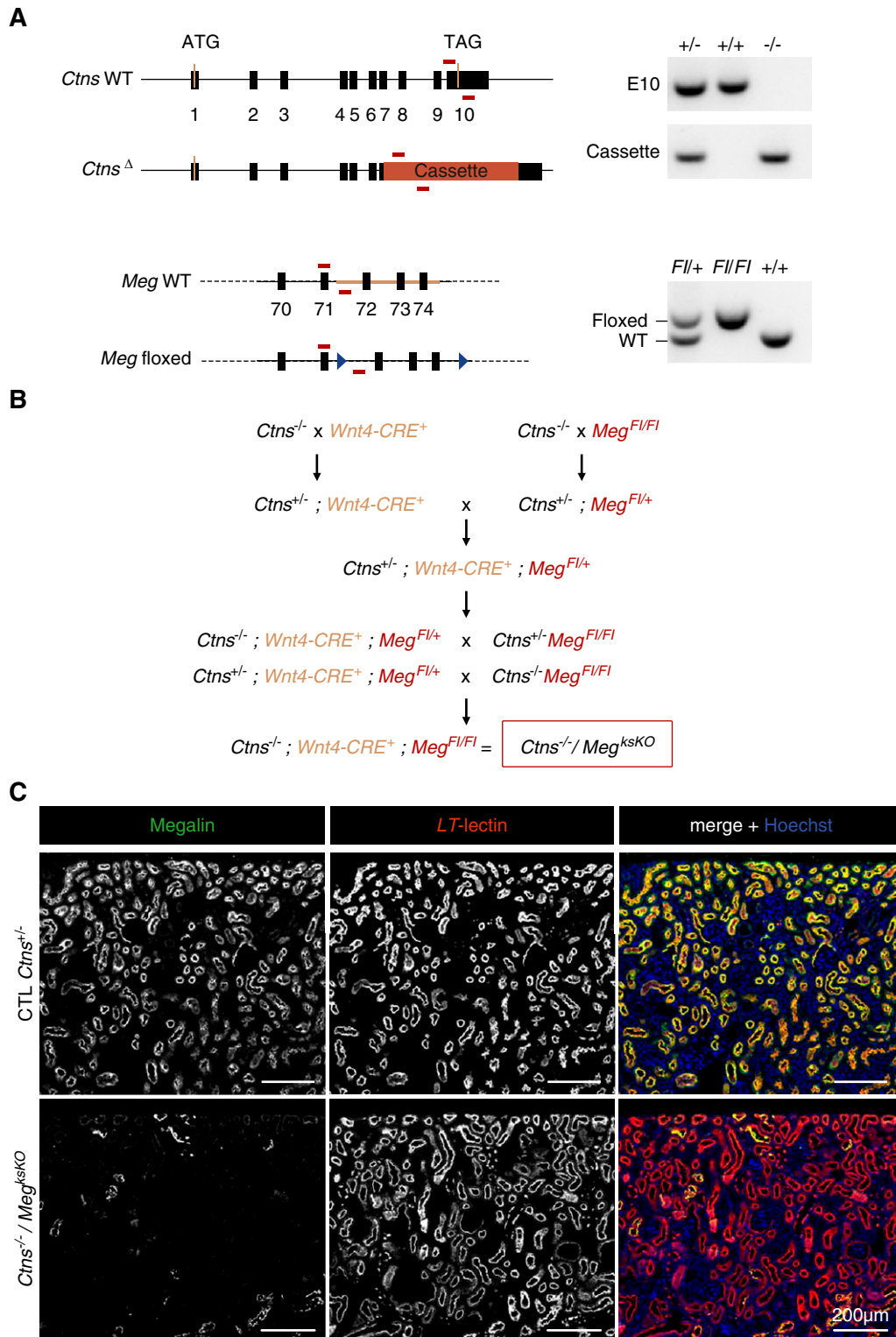


Figure 1. Generation and validation of *Ctns*/*Meg* double KO in kidneys. (A) Genotyping: *Cystinosis* and *megalyn* floxed alleles were identified by PCR on tail DNAs. For *cystinosis*, WT exon 10 (E10) or cassette (IRES- β gal-neo) replacing the last four exons (vertical black bars) of *Ctns* were amplified with two different oligonucleotides pairs (horizontal red bars), allowing for identification of WT, heterozygous, and *Ctns*^{-/-} mice. For *megalyn*, a common forward oligonucleotide was used with two different reverse oligonucleotides specific to the WT or floxed allele, containing *LoxP* recombination sites (blue triangles). Amplification of the *Wnt4*-*CRE* locus is not depicted. (B) Crossings: This crossing program aimed at comparing mice with various genotypes strictly derived from the same

bright-field microscopy, with a polarizing filter added between the light source and the condenser, and a Wollaston prism to increase the contrast. Alternatively, whole kidney images (histology and fluorescence) were acquired using a Panoramic 250 Flash III microscope (3DHitech).

At least four mice were analyzed for each condition. Swan-neck morphometry was performed by survey of an entire sagittal section across the hilum. In 32 such sections (including all controls, single KOs, and double KOs except the case mentioned hereafter), on average 21 ± 8 GTJs per section were identified (mean \pm SD, range 8–36). One double KO mouse at 9 months with less than five GTJs identified was rejected. Comparison of the three groups by Mann–Whitney test showed no significant difference in GTJ abundance, but significant difference in frequency of swan-necks (Supplemental Methods).

Statistical Analysis

All statistical analyses were conducted by Prism software (GraphPad Software) using the nonparametric Mann–Whitney test. Differences were considered statistically significant when $P < 0.05$.

RESULTS

Wnt4-CRE-Driven, Kidney-Specific Megalin Ablation in Cystinosis KO Mice and Validation of the Model

The breeding program used to achieve triple transgenic mice ($Ctns^{-/-}/Meg^{ksKO}$ or double KO), genotyped as shown at Figure 1A, is outlined at Figure 1B. Because the cystinotic renal phenotype in $Ctns$ KO mice strongly depends on genetic background,³¹ breeding was designed to compare kidneys of “control” ($Ctns^{+/+}$), single $Ctns$ KO ($Ctns^{-/-}$), single $ksMeg$ KO ($Wnt4-CRE; Meg^{F1/F1}$), and double KO ($Ctns^{-/-}; Wnt4-CRE; Meg^{F1/F1}$) mice derived from the same C57BL/6J founders. Genotypes of all offspring followed expected Mendelian proportions. There was no significant difference in body growth or kidney weight between all genotypes up to 9 months (longest endpoint; Supplemental Figure 1), indicating phenotype attenuation since the original report.³¹ At the time of euthanasia, urinary signs of partial Fanconi syndrome, previously reported to discriminate $Ctns^{-/-}$ mice from control littermates,^{26,31} were no longer found, which was also noticed in $Ctns^{-/-}$ colonies at other laboratories. There was also no significant alteration in urea and creatinine plasma values, except for increased mean urea in double KO

mice at 9 months (74.5 ± 26.0 mg/dl, $P < 0.05$ versus 54.6 ± 8.1 in control and $P < 0.05$ versus 51.2 ± 11.6 in $Ctns^{-/-}$; means \pm SD). This paradoxical increase will be explained hereafter. Confocal immunofluorescence, using proximal tubule-specific labeling by *L. tetragonolobus* lectin as a reference, showed almost complete disappearance of megalin expression in double KO PTCs (Figures 1C and 2C). Thus, $Ctns^{-/-}/Meg^{ksKO}$ mice appeared adequate to test the role of endocytosis in the progression of kidney lesions in cystinotic mice. However, histology revealed in the cortex of about half, but not all, single $ksMeg$ KO and double KO mice massive periarterial lymphocyte collections and extending inflammation, causing large zones with gross tissue remodeling after 6 months (see further in Figure 3 and Supplemental Figure 6, A and B). These mice were not excluded from the assays but conclusions reported hereafter for double KO were validated for mice without such extensive remodeling zones.

Megalin Ablation in $Ctns^{-/-}$ Kidneys Blocks Cystine Accumulation in Lysosomes and Prevents Crystal Deposition

To assess whether suppressing endocytosis into PTCs by genetic megalin ablation would prevent cystine accumulation, we first performed cystine assays in kidneys at 6, 7.5, and 9 months of age in each genotype. At all time points, renal cystine levels in $Ctns^{-/-}$ mice were significantly different from control ($Ctns^{+/+}$, $Ctns^{+/-}$) and single $ksMeg$ KO mice (Supplemental Figure 2). We thus focused on the comparison of renal cystine levels between $Ctns^{-/-}$ and double KO mice. As positive controls of cystinosis and negative controls of megalin ablation, we also assayed cystine in liver and spleen, in which the *Wnt4* gene is not expressed (Figure 2A, Supplemental Figure 2). In $Ctns^{-/-}$ kidneys, cystine accumulation increased exponentially with age, reaching on average 103 nmol hemi-cystine/mg tissue protein at 9 months, in good agreement with Nevo *et al.*,³¹ but this leveled off at 13 nmol hemi-cystine/mg tissue protein in double KO kidneys. Thus, kidney-specific megalin gene ablation in $Ctns^{-/-}$ almost entirely suppressed kidney cystine overload. In contrast, there was no consistent change in cystine levels in spleen or liver. Suppression of cystine accumulation could not be explained by modifier genes associated with Meg^{F1} or *Wnt4-CRE* loci, because two double transgenic $Ctns^{-/-}; Meg^{F1/F1}$ mice and at least one $Ctns^{-/-}; Wnt4-CRE$ mouse—all expected to express megalin normally—still showed high kidney cystine levels (red or green color code in Figure 2A). In $Ctns^{-/-}$

founders. Offspring were observed at the expected Mendelian proportions. (C) Validation of *Wnt4-CRE*-driven excision of megalin in double KO mice by double confocal fluorescence (6 months): Low-power view for megalin immunofluorescence in green, and apical labeling of PTCs by *L. tetragonolobus* lectin (LT-lectin) in red. Single channels at left and center, merged emission at right combined with nuclear labeling by Hoechst (blue). As compared with control (CTL; all labeled tubular sections appear yellow), note the almost complete disappearance of megalin in double KO (very few yellow tubular sections).

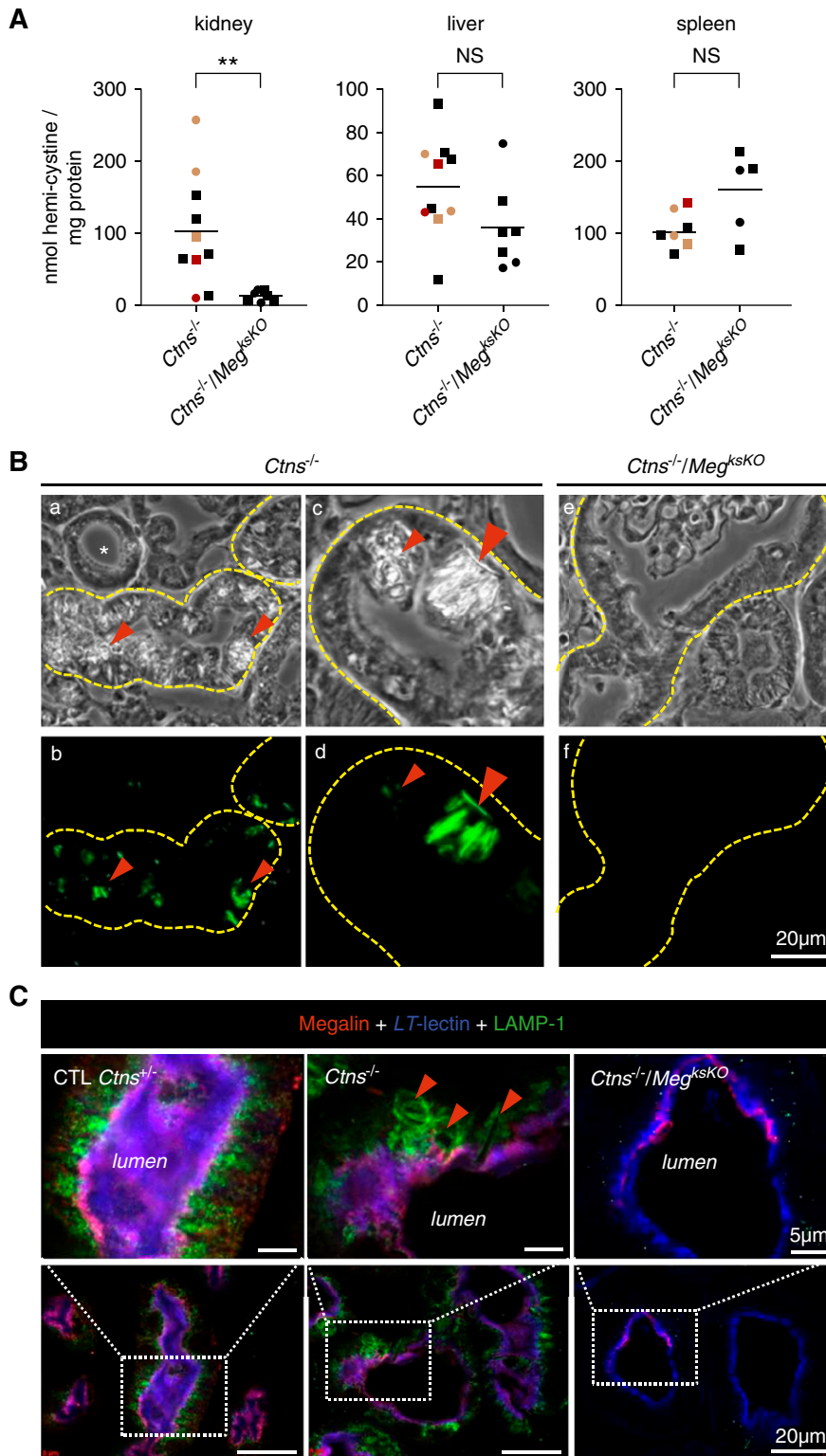


Figure 2. Megalin ablation in *Ctns*^{-/-} kidneys prevents cystine accumulation and crystal deposition. (A) Comparison of cystine content in kidneys, liver, and spleen between *Ctns*^{-/-} and double KO mice at 9 months of age for males (filled squares) or females (filled circles) (***P*<0.01). Red and orange symbols refer to *Ctns*^{-/-} mice with either two floxed *megal*in alleles but no *Wnt4*-CRE, or one *Wnt4*-CRE but no floxed *megal*in allele, respectively. For time course of cystine accumulation between 6 and 9 months, see Supplemental Figure 2. (B) Histologic evidence of cystine crystals (red arrowheads) by polarized light (top panel) and green pseudo-color (bottom panel) in *Ctns*^{-/-} kidneys (a, b, c, d) versus their absence in double KO kidneys at 7.5 months (e, f). For large fields, see Supplemental

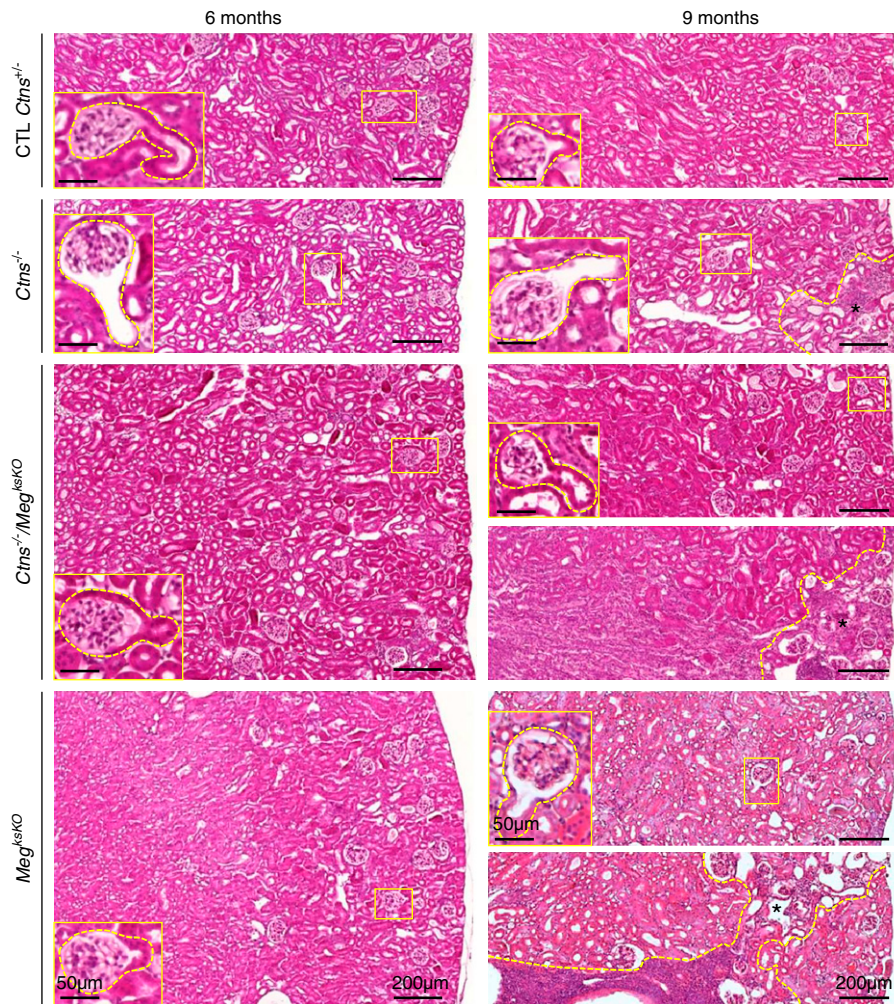


Figure 3. Histology of cystinotic kidneys is preserved upon *megalín* ablation (whole-cortical views after staining with hematoxylin and eosin at 6 and 9 months). Broken yellow lines delineate inflammatory areas with parenchymal atrophy at 9 months (*). Representative GTJs are enlarged. In single *Ctns*^{-/-} KO mice at 9 months, small foci of atrophy are always present but limited to the superficial cortex. For double KO and single *Meg*^{ksKO} KO kidneys at 9 months, two examples are shown to illustrate either absence or presence of grossly remodeled areas that can span the entire cortex (see also Supplemental Figure 6B). CTL, control.

PTCs, lysosomal cystine accumulation results in lysosomal swelling and then deformities due to cystine crystallization at the acidic lysosomal pH.^{26,31} Cystine crystals, readily evidenced in *Ctns*^{-/-} PTCs by polarized microscopy, were no longer detected upon megalin ablation (Figure 2B, Supplemental Figure 3). Of note, no crystals were detected in atrophic *Ctns*^{-/-} PTCs at swan-neck deformities.

Moreover, lysosome labeling by LAMP-1 immunofluorescence revealed frequent lysosomal dilation and characteristic deformation by crystals in *Ctns*^{-/-} PTCs but never in *Ctns*^{-/-}/*Meg*^{ksKO}, indicating protection against lysosomal abnormalities (Figure 2C). Altogether, these data demonstrated that genetic abrogation of apical endocytosis into *Ctns*^{-/-} PTCs was very efficient in preventing cystine accumulation,

Figure 3. (C) Triple confocal fluorescence imaging of *N*-fucosyl glycosides (LT-lectin, blue), megalin (red), and late-endosome/lysosome membrane (LAMP-1, green) at 6 months. In control PTCs, brush border is uniformly purple (combined blue and red emissions); lysosomes are all round and of similar size. In *Ctns*^{-/-} PTCs, notice several enlarged and deformed lysosomes due to cystine crystal buildup (red arrowheads); brush border is preserved here. In double KO PTCs, brush border is only labeled in blue in most cells, reflecting megalin absence, and LAMP-1 signal is much reduced by comparison with controls as a consequence of abrogation of endocytic uptake. *LT*-lectin, *L. tetragonolobus* lectin.

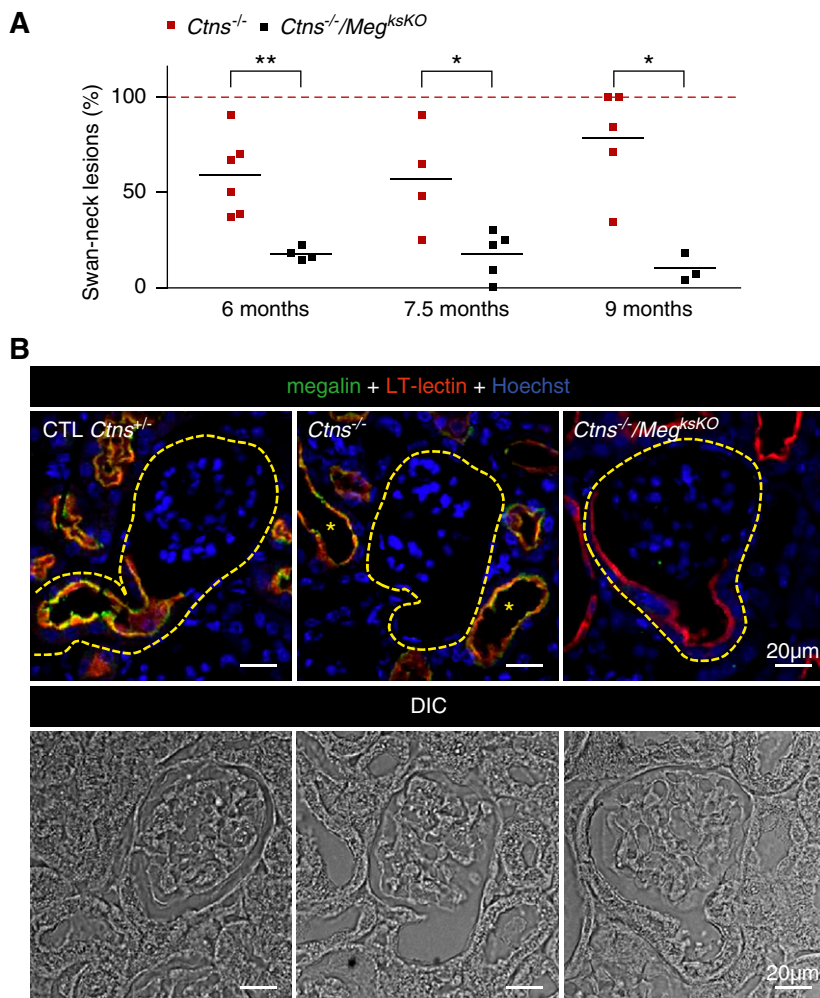


Figure 4. *Megalin* ablation in *Ctns*^{-/-} kidneys prevents swan-neck lesions at GTJs. (A) Quantification of swan-neck lesions in *Ctns*^{-/-} versus double KO mice from 6 to 9 months of age as percentage of all well defined GTJs over the entire sagittal kidney section, except at large inflammatory zones, as illustrated at Figure 3. **P*<0.05, ***P*<0.01, nonparametric Mann–Whitney test). (B) Triple fluorescence confocal imaging with reference to differential interference contrast (DIC) imaging in *Ctns*^{-/-} versus double KO mice at 6 months of age for *L. tetragonolobus* lectin (LT-lectin) labeling (red) and megalin (green) combined with nuclear Hoechst labeling (blue). Contours of GTJs are delineated by yellow broken lines. Notice in the central image that megalin is not detected at this representative *Ctns*^{-/-} GTJ due to dedifferentiation/atrophy, but is preserved in more distal PTCs, together with LT-lectin labeling (yellow *). In contrast, the right image shows that megalin inactivation in *Ctns*^{-/-} kidneys (no green signal) generally preserves PTC thickness and LT-lectin labeling at the GTJ. CTL, control.

indicating the endocytic pathway is indeed the key source of cystine storage in nephropathic cystinosis.

Megalin Ablation in *Ctns*^{-/-} Kidneys Preserves Proximal Tubular Structure

As in cystinotic children,²³ mouse *Ctns*^{-/-} kidneys show typical swan-neck lesions after 6 months.^{26,27} To determine whether *Megalin* ablation would further protect the proximal

tubule structure, we compared double KO with *Ctns*^{-/-} full-kidney sagittal sections by histology after staining with hematoxylin and eosin (Figure 3, quantified in Figure 4A) and by plastic sections of smaller blocks after toluidine-blue staining (Supplemental Figure 4). The majority of GTJs in *Ctns*^{-/-} kidneys from 6–9 months of age showed typical swan-neck lesions, with apparently increasing prevalence with age, in good agreement with morphometry by Galarreta *et al.*²⁷ In contrast, only approximately 20% of GTJs in double KO showed swan-neck pattern without increase in age. This conclusion was confirmed by confocal microscopy based on *L. tetragonolobus* lectin labeling, as a general apical proximal tubule marker for brush border and apical endocytic apparatus, combined with megalin immunofluorescence. In control mice, double labeling produced a yellow signal. In *Ctns*^{-/-} kidneys, both signals were suppressed at most GTJs and downstream. In double KO PTCs, lectin labeling was largely preserved (Figure 4B). Thus, *Megalin* ablation in *Ctns*^{-/-} kidney protected against overall PTC dedifferentiation and atrophy. Electron microscopy confirmed the preservation of double KO PTCs, except for atrophy of the apical endocytic apparatus and paucity of lysosomes, which was also the case in single *Meg*^{ksKO} KOs (Supplemental Figure 5).

Megalin Ablation in *Ctns*^{-/-} Kidneys Preserves the Apical Expression of NaPi-IIa and SGLT-2 in PTCs and Prevents Increased PTC Turnover

Dedifferentiation of cystinotic PTCs, starting at the GTJ, includes loss of expression of megalin and cubilin, as well as of the main sodium-phosphate symporter, NaPi-IIa, and the main sodium-glucose symporter, SGLT-2, which are all relevant to Fanconi syndrome.²⁶ Because swan-neck lesions are considered an early adaptation to PCT insult,^{26,27} we next addressed whether double

double KO PTCs would escape this defensive mechanism. As shown by immunolabeling for NaPi-IIa (Figure 5A) and SGLT-2 (Figure 5B), all *Ctns*^{-/-} cortices showed diffuse loss of expression of both transporters, yielding a mottled appearance at low magnification, but double KO preserved expression, except at large inflammatory areas where histology was grossly altered (for whole-cortical views, see Supplemental Figure 6, A and B). Because urinalysis of Fanconi syndrome

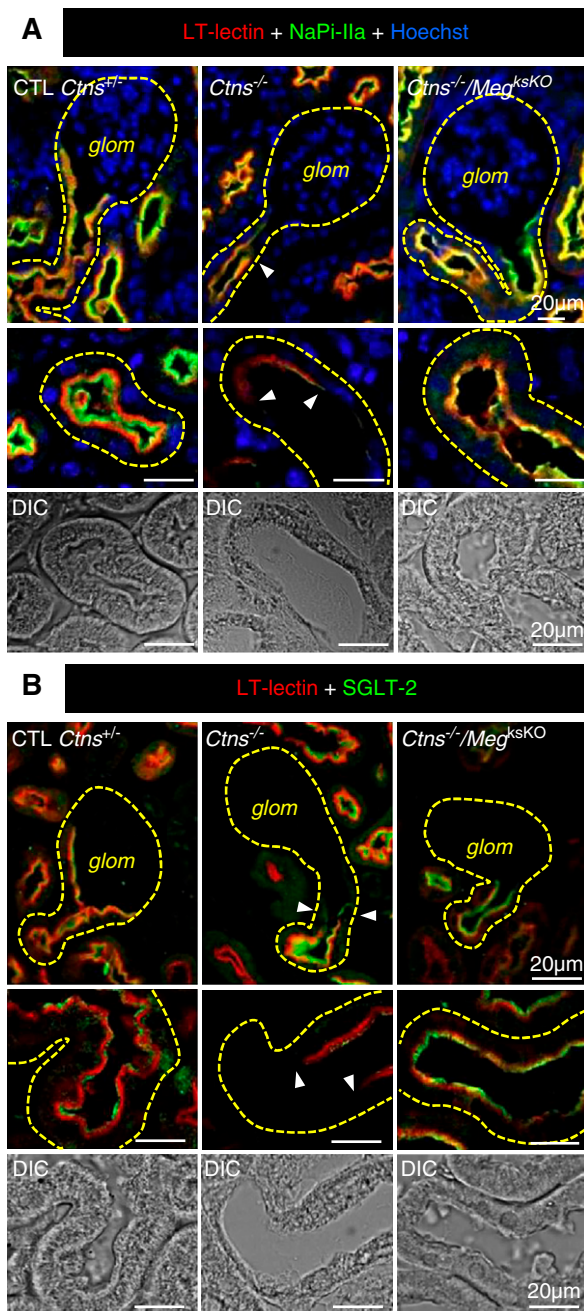


Figure 5. Protection against apical dedifferentiation in double KO kidneys. Double (or triple, Hoechst in blue) confocal fluorescence at 6 months for *L. tetragonolobus* lectin (LT-lectin) labeling (red), and either (A) NaPi-IIa or (B) SGLT-2 in green. Top panels, GTJs; bottom panels, enlargement of representative proximal tubule sections. On the left, notice in control (CTL) PTCs restriction of NaPi-IIa and SGLT-2 to the brush border but extension of LT-labeling subapically, resulting in apical label stratification. In *Ctns*^{-/-} PTCs (central panels), LT-lectin and NaPi-IIa or SGLT-2 signals are greatly decreased or absent (arrowheads indicate sharp boundary with preserved cells). On the right, *megalina* ablation in *Ctns*^{-/-} kidneys preserves apical signal of LT-lectin and NaPi-IIa or SGLT-2; stratification is lost due to atrophy of subapical endocytic apparatus. For whole-cortex views, see Supplemental Figure 6, A and B. For RT-PCR, see Supplemental Figure 7. DIC, differential interference contrast; glom, glomerulus.

was no longer relevant due to loss of this phenotype in our *Ctns*^{-/-} colony, we performed quantitative RT-PCR measurements of cubilin, NaPi-IIa, and SGLT-2 mRNAs at 9 months (Supplemental Figure 7). There was a consistent decreasing trend in *Ctns*^{-/-} kidneys as compared with control littermates, in agreement with previous reports,^{26,32} contrasting with apparent protection in double KO, although differences did not reach statistical significance. Altogether, immunofluorescence and quantitative RT-PCR data were compatible with the hypothesis that the Fanconi syndrome of nephropathic cystinosis could be attenuated by targeting the megalin pathway.

Another adaptation mechanism to cystine overload in *Ctns*^{-/-} PTCs is cell death, including by apoptotic shedding leading to luminal crystal discharge, coupled with compensatory proliferation, *i.e.*, replenishment by dividing cells to yield fresh lysosomes.²⁶ In contrast to *Ctns*^{-/-} cortices, apoptosis and proliferation (monitored by cleaved caspase-3 and Ki-67 immunofluorescence, respectively) were not detectably increased in double KO cortices, indicating no change in PTC turnover (Figure 6). Thus, *megalina* ablation in cystinotic kidneys, which suppressed exogenous cystine supply, also normalized apoptosis and proliferation rates.

DISCUSSION

This report demonstrates genetic ablation of the megalin/LRP2 pathway in cystinotic kidneys (1) suppresses cystine accumulation and crystal deposition, (2) protects tissue structure (except for grossly remodeled areas), and (3) preserves PTC differentiation and presumably function. This benefit was observed throughout the kidney cortex outside of those grossly remodeled areas, as expected from early *Wnt4-CRE*-driven excision, and is consistent with megalin being the cornerstone for PTC endocytosis in S1 (and S2) segments.^{6,7,43} Using *Wnt4-CRE*, double *megalina/cubilin* KO causes higher albuminuria than single *megalina* KO (1.5-fold) and single cubilin KO (threefold).⁹ However, full inhibition of endocytosis is not needed for a major benefit on cystine level in cystinotic PTCs, because a significant fraction of cystine released in lysosomes can be further disposed of by apical vesicular efflux (discussed in²⁴). Conversely, side effects like suppressed endocytic supply of potential nephroprotective proteins, such as iron siderophore neutrophil gelatinase-associated lipocalin⁴⁴ or survivin,⁴⁵ must be taken into account and could explain the 20% of swan-neck lesions in double KO kidneys. Alternatively, these residual lesions could be due to a defective nontransport function of cystinosin. Perinatal ablation of the megalin pathway, used here as an experimental artifact, should not be confused with the natural course of nephropathic cystinosis where receptor-mediated endocytosis in S1/S2 spontaneously declines after 3–6 months as part of adaptive dedifferentiation to decrease workload.^{26,27,32} Conceivably, secondary attenuation of apical endocytosis might be mediated by impaired mTOR signaling

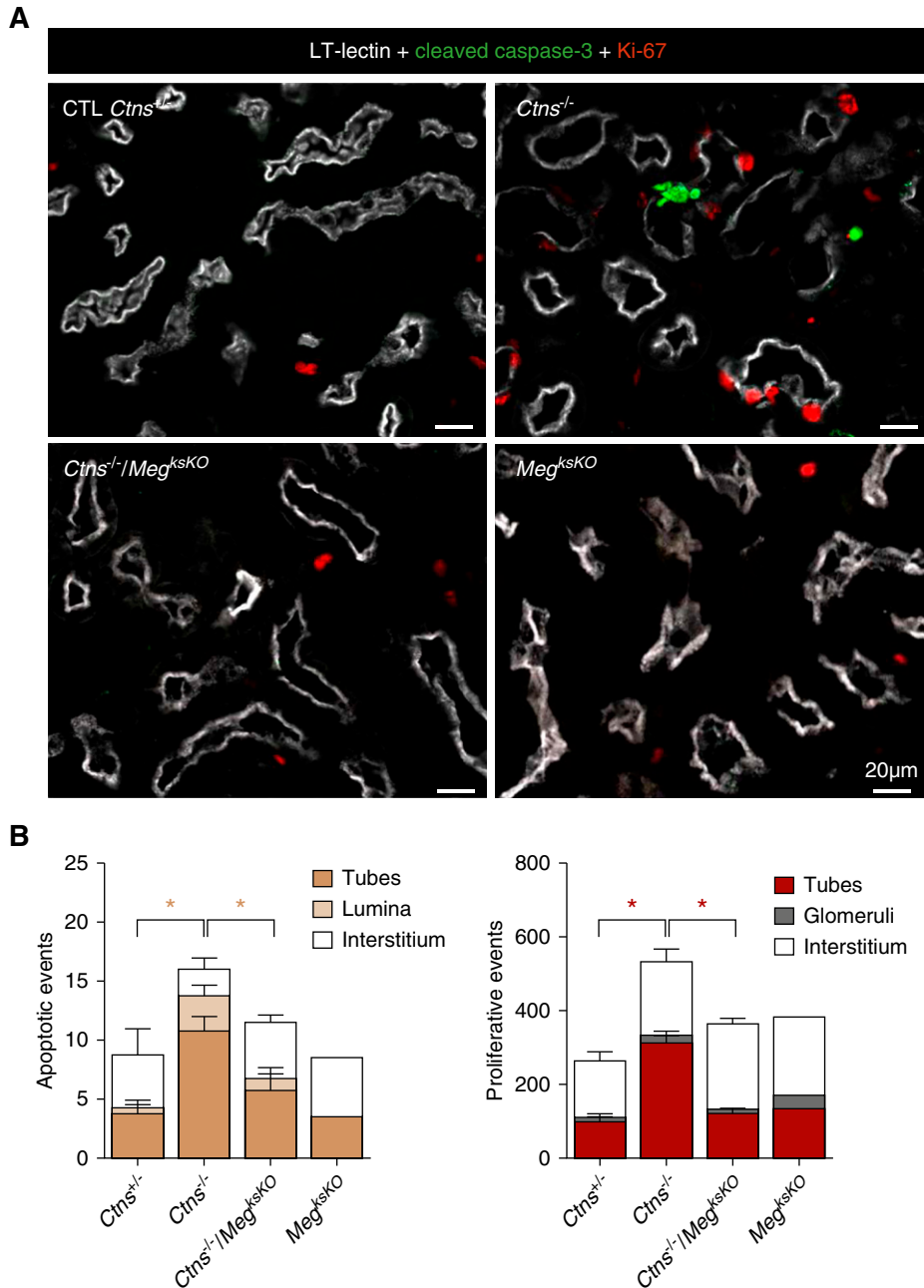


Figure 6. Megalin ablation in *Ctns*^{-/-} kidneys protects against apoptosis and prevents increased PTC turnover. (A) Triple fluorescence confocal imaging for *L. tetragonolobus* lectin (LT-lectin) signal as proximal tubule marker (represented in white), caspase-3a (cleaved, active caspase-3) as apoptotic marker (green), and Ki-67 as proliferation marker (red) in representative low-power views. Notice increased labeling for both markers in *Ctns*^{-/-} but not double KO kidneys. (B) PTC turnover quantification. Cells labeled for caspase-3a or Ki-67 were counted in kidney sections at 6 months (four mice in *Ctns*^{+/+}, *Ctns*^{-/-}, and *Ctns*^{-/-}/*Meg*^{ksKO}; two mice for *Meg*^{ksKO}; ten random cortical fields totaling 2.98 mm² per section). Statistical analysis of the significance of differences of frequencies in tubes (combined with lumina for apoptosis) by Mann–Whitney test, **P*<0.05. Increased apoptotic and proliferation indices in *Ctns*^{-/-} kidneys indicate accelerated PTC turnover, not observed in double KO. CTL, control.

due to absence of cystinosin,³⁷ which negatively affects the apical endocytic machinery.⁶ Conversely, nonrecaptured disulfide-rich proteins are reclaimed by more distal cells, which in turn get affected.²⁶ This would readily explain distal/longitudinal disease extension (see Visual Abstract).

Megalin/LRP2 ablation in mice and in-depth study of patients with Donnai–Barrow syndrome⁴⁶ (who have genetic *megalin/LRP2* deficiency) were instrumental in establishing its multiple roles in kidney physiology (reviewed in ⁴⁷). Endocytic receptor KO models have also been essential to revise

or refine concepts involving the role of proteinuria as a risk factor to kidney insufficiency⁴⁸ or the still-debated albumin transcytotic recycling route.⁴⁹ Here, *megalyn* KO revealed that endocytosis is the major pathway for the accumulation of cystine in nephropathic cystinosis, and provided proof of concept for the megalin pathway as therapeutic target. Because the kidney phenotype in *Ctns*^{-/-} mice critically depends on the genetic background, we ensured that we compared mice derived from the same founders and excluded a role of floxed *megalyn* and *Wnt4-CRE* loci. This concern was particularly important for the *Wnt4-CRE* locus because the gene coding for CdC42, key regulator of apical differentiation, lies immediately behind the *Wnt4* gene on *Mus musculus* chromosome 4, locus D3. A limitation of our study is the inflammatory/immune reaction causing gross tissue remodeling in approximately half of mice at 9 months. This unexplained side effect of *Wnt4-CRE*-driven *megalyn* excision (not reported in other, less complete, megalin KO models) likely explains the paradoxical increase (and large variation) of average plasma urea concentration in double KO mice at 9 months. However, the resulting gross remodeling is very different from the diffuse mottled appearance in *Ctns*^{-/-} kidneys. Moreover, cortex between extensively remodeled areas in affected double KO mice as well as the entire cortex in double KO mice without remodeling showed remarkable structural protection. Thus, we feel it is safe to conclude that structural protection in double KO mice could be attributed to genetic ablation of the megalin pathway, and that suppression of this pathway by other means, not inducing gross inflammatory remodeling, could represent a desirable objective.

Our starting hypothesis was that receptor-mediated endocytosis of ultrafiltrated, disulfide-rich plasma proteins—exemplified by, but not limited to, albumin—was the main cystine source of PTCs. However, calculations indicate the much higher concentrations of free as compared with protein-bound cystine in the primary ultrafiltrate (approximately two orders of magnitude higher) may balance the much lower efficiency of fluid-phase versus receptor-mediated endocytosis (approximately two orders of magnitude lower)^{50,51} so that contribution of fluid-phase endocytosis to cystine supply²¹ into normal PTCs cannot be *a priori* neglected. Moreover, because megalin ablation not only arrests receptor-mediated endocytosis but also causes a marked atrophy of the apical endocytic apparatus and impairs fluid-phase endocytosis,¹² data in this report do not allow us to discriminate the two modes of endocytosis. The term “megalyn pathway” used here intends to cover both mechanisms. Further studies, *e.g.*, by direct megalin competition for protein binding, are necessary to clarify this issue.

Acute suppression of the megalin pathway can be achieved by inhibition with dibasic amino acids, as shown with cultured cells^{16,52} and by bolus injection into human volunteers,¹⁵ perfusion in patients with cancer to prevent nephrotoxicity of radiochemicals,⁵³ or oral gavage in rats.¹⁶ Long-term supplementation with arginine in man is considered safe,⁵⁴ is part

of the treatment of genetic diseases of the urea cycle,⁵⁵ and is commonly used by body builders. Long-term supplementation with lysine is used for prevention of gyrate atrophy in hereditary ornithinemia.⁵⁶ Preliminary data from our laboratory have shown that dietary supplementation of *Ctns*^{-/-} mice by L-lysine or L-arginine can significantly decrease kidney cystine accumulation and swan-neck lesions. However, dibasic amino acids can affect several metabolic pathways⁵⁷ and have several potential cellular targets, such as direct competition for receptor binding, inhibition of endocytic trafficking, and/or stimulation of the mTOR pathway⁵⁸ which is defective in cystinotic cells.³⁷ Thus, besides the need for confirmation in large cohorts, further mechanistic studies are required to clarify the mechanism of protection upon long-term supplementation.

The respective roles in the pathogeny and manifestations of nephropathic cystinosis of cystine transport-dependent (defined as cysteamine-responsive) versus transport-independent (cysteamine-insensitive, reviewed in²⁴) functions of cystinosis, is also unknown. Cysteamine insensitivity of Fanconi syndrome contrasts with improved kidney outcome upon early compliant drug implementation.^{30,59} Delayed progression to kidney insufficiency stresses the importance of effective cystine kidney clearance, although actual level of depletion, inferred from leukocyte assays, may not be complete in kidneys, as suggested in cysteamine-treated *Ctns*^{-/-} mice.⁶⁰ Our article sheds more light on this debate by evidencing a causal link between cystine accumulation and structural dedifferentiation of PTCs in the mouse model, because prevention of cystine overload correlated with structural preservation; thus these results somewhat swing the pendulum back toward the pathogenic role of cystine overload.

ACKNOWLEDGMENTS

We thank Dr. R. Kozyraki and Dr. P. Verroust for anti-megalyn and anti-cubilin antibodies, as well as Dr. J. Biber and Dr. C. Wagner for anti-Na-Pi-IIa antibodies; they are outstanding reagents. We express our gratitude to Dr. P. Henriot for supervision of statistical tests and *in silico* analysis of genomic DNA around *cystinosis*, *megalyn*, and *Wnt4* loci. We are particularly grateful to the wise reviewer who suggested considering fluid-phase endocytosis of free cystine as an additional mechanism to receptor-mediated endocytosis.

Janssens, Pierreux, and Courtoy designed the study; Nevo, Vainio, Nielsen, Christensen, and Antignac provided mice; Janssens, Gaide Chevronnay, Marie, Vincent, and Jouret carried out experiments; Van Der Smissen performed electron microscopy. Janssens, Gaide Chevronnay, Nielsen, Christensen, Jouret, Antignac, Pierreux, and Courtoy analyzed the data; Janssens and Courtoy created the figures; Janssens, Pierreux, and Courtoy drafted and revised the paper; all authors approved the final version of the manuscript.

Gaïde Chevronnay was a postdoctoral researcher and Pierreux is a senior research associate at Fonds de la Recherche Scientifique, Fonds National de la Recherche Scientifique (F.R.S.–FNRS). Jouret is a PhD postdoctoral fellow of the F.R.S.–FNRS, Belgium.

DISCLOSURES

Work performed by Courtoy, Gaïde Chevronnay, Janssens, Marie, Pierreux, Van Der Smissen, and Vincent was supported by grants from the Cystinosis Research Foundation (CRF).

FUNDING

This study was supported by the CRF (running costs, Janssens salary). The Imaging Cells and Tissues core facility was financed by National Lottery, Région bruxelloise, Région wallonne, Université Catholique de Louvain and de Duve Institute.

SUPPLEMENTAL MATERIAL

This article contains the following supplemental material online at <http://jasn.asnjournals.org/lookup/suppl/doi:10.1681/ASN.2019040371/-/DCSupplemental>.

Supplemental Methods. Semi-thin sections and electron microscopy RT-PCR.

Supplemental Figure 1. Time-course of body and kidney weight.

Supplemental Figure 2. Megalin ablation in *Ctns*^{-/-} kidneys selectively prevents cystine accumulation (complementary to Figure 2A).

Supplemental Figure 3. Megalin ablation in *Ctns*^{-/-} kidneys prevents cystine crystal deposition: gallery of images (complementary to Figure 2B).

Supplemental Figure 4. Toluidine-stained plastic sections of *Ctns*^{-/-} vs double KO kidneys.

Supplemental Figure 5. Electron microscopy.

Supplemental Figure 6. Diffuse mottled appearance resulting from loss of transporter expression in *Ctns*^{-/-} PCTs contrasts with large areas of inflammatory remodelling in double KO. (A) Low power cortical views. (B) Extended views of whole kidney sections (complementary to Figure 5).

Supplemental Figure 7. RT-PCR of megalin, cubilin, NaPi-IIa and SGLT-2.

Supplemental References.

REFERENCES

- Christensen EI, Wagner CA, Kaissling B: Uriniferous tubule: Structural and functional organization. *Compr Physiol* 2: 805–861, 2012
- Eshbach ML, Weisz OA: Receptor-mediated endocytosis in the proximal tubule. *Annu Rev Physiol* 79: 425–448, 2017
- Christensen EI, Birn H: Megalin and cubilin: Multifunctional endocytic receptors. *Nat Rev Mol Cell Biol* 3: 256–266, 2002
- Birn H, Christensen EI, Nielsen S: Kinetics of endocytosis in renal proximal tubule studied with ruthenium red as membrane marker. *Am J Physiol* 264: F239–F250, 1993
- Perez Bay AE, Schreiner R, Benedicto I, Paz Marzolo M, Banfelder J, Weinstein AM, et al.: The fast-recycling receptor Megalin defines the apical recycling pathway of epithelial cells. *Nat Commun* 7: 11550, 2016
- Grahammer F, Ramakrishnan SK, Rinschen MM, Larionov AA, Syed M, Khatib H, et al.: mTOR regulates endocytosis and nutrient transport in proximal tubular cells. *J Am Soc Nephrol* 28: 230–241, 2017
- Schuh CD, Polesel M, Platonova E, Haenni D, Gassama A, Tokonami N, et al.: Combined structural and functional imaging of the kidney reveals major axial differences in proximal tubule endocytosis. *J Am Soc Nephrol* 29: 2696–2712, 2018
- Amsellem S, Gburek J, Hamard G, Nielsen R, Willnow TE, Devuyst O, et al.: Cubilin is essential for albumin reabsorption in the renal proximal tubule. *J Am Soc Nephrol* 21: 1859–1867, 2010
- Weyer K, Storm T, Shan J, Vainio S, Kozyraki R, Verroust PJ, et al.: Mouse model of proximal tubule endocytic dysfunction. *Nephrol Dial Transplant* 26: 3446–3451, 2011
- Willnow TE, Hilpert J, Armstrong SA, Rohlmann A, Hammer RE, Burns DK, et al.: Defective forebrain development in mice lacking gp330/megalin. *Proc Natl Acad Sci U S A* 93: 8460–8464, 1996
- Lehste JR, Rolinski B, Vorum H, Hilpert J, Nykjaer A, Jacobsen C, et al.: Megalin knockout mice as an animal model of low molecular weight proteinuria. *Am J Pathol* 155: 1361–1370, 1999
- Bachmann S, Schlichting U, Geist B, Mutig K, Petsch T, Bacic D, et al.: Kidney-specific inactivation of the megalin gene impairs trafficking of renal inorganic sodium phosphate cotransporter (NaPi-IIa). *J Am Soc Nephrol* 15: 892–900, 2004
- Schmitz C, Hilpert J, Jacobsen C, Boensch C, Christensen EI, Luft FC, et al.: Megalin deficiency offers protection from renal aminoglycoside accumulation. *J Biol Chem* 277: 618–622, 2002
- Hori Y, Aoki N, Kuwahara S, Hosojima M, Kaseda R, Goto S, et al.: Megalin blockade with cilastatin suppresses drug-induced nephrotoxicity. *J Am Soc Nephrol* 28: 1783–1791, 2017
- Mogensen CE, Sølling: Studies on renal tubular protein reabsorption: Partial and near complete inhibition by certain amino acids. *Scand J Clin Lab Invest* 37: 477–486, 1977
- Thelle K, Christensen EI, Vorum H, Ørskov H, Birn H: Characterization of proteinuria and tubular protein uptake in a new model of oral L-lysine administration in rats. *Kidney Int* 69: 1333–1340, 2006
- Gahl WA, Thoene J, Schneider JA: Cystinosis: a disorder of lysosomal membrane transport. In: *The metabolic and molecular bases of inherited disease*, Vol. 3, edited by Scriver CR, Beaudet AL, Sly WS, Valle D, New York, NY, McGraw Hill, 2001, pp 5085–5108
- Lloyd JB: Disulphide reduction in lysosomes. The role of cysteine. *Biochem J* 237: 271–272, 1986
- Thoene JG, Lemons RM: Cystine accumulation in cystinotic fibroblasts from free and protein-linked cystine but not cysteine. *Biochem J* 208: 823–830, 1982
- Thoene JG, Lemons R: Modulation of the intracellular cystine content of cystinotic fibroblasts by extracellular albumin. *Pediatr Res* 14: 785–787, 1980
- Thoene JG, Forster S, Lloyd JB: The role of pinocytosis in the cellular uptake of an amino acid. *Biochem Biophys Res Commun* 127: 733–738, 1985
- Wilmer MJ, Emma F, Levchenko EN: The pathogenesis of cystinosis: Mechanisms beyond cystine accumulation. *Am J Physiol Renal Physiol* 299: F905–F916, 2010
- Mahoney CP, Striker GE: Early development of the renal lesions in infantile cystinosis. *Pediatr Nephrol* 15: 50–56, 2000
- Cherqui S, Courtoy PJ: The renal Fanconi syndrome in cystinosis: Pathogenic insights and therapeutic perspectives. *Nat Rev Nephrol* 13: 115–131, 2017
- Larsen CP, Walker PD, Thoene JG: The incidence of atubular glomeruli in nephropathic cystinosis renal biopsies. *Mol Genet Metab* 101: 417–420, 2010
- Gaïde Chevronnay HP, Janssens V, Van Der Smissen P, N’Kuli F, Nevo N, Guiot Y, et al.: Time course of pathogenic and adaptation

- mechanisms in cystinotic mouse kidneys. *J Am Soc Nephrol* 25: 1256–1269, 2014
27. Galarreta CI, Forbes MS, Thornhill BA, Antignac C, Gubler MC, Nevo N, et al.: The swan-neck lesion: Proximal tubular adaptation to oxidative stress in nephropathic cystinosis. *Am J Physiol Renal Physiol* 308: F1155–F1166, 2015
 28. Kleta R, Bernardini I, Ueda M, Varade WS, Phornphutkul C, Krasnewich D, et al.: Long-term follow-up of well-treated nephropathic cystinosis patients. *J Pediatr* 145: 555–560, 2004
 29. Cherqui S: Cysteamine therapy: A treatment for cystinosis, not a cure. *Kidney Int* 81: 127–129, 2012
 30. Emma F, Nesterova G, Langman C, Labbé A, Cherqui S, Goodyer P, et al.: Nephropathic cystinosis: An international consensus document. *Nephrol Dial Transplant* 29[Suppl 4]: iv87–iv94, 2014
 31. Nevo N, Chol M, Bailleux A, Kalatzis V, Morisset L, Devuyst O, et al.: Renal phenotype of the cystinosis mouse model is dependent upon genetic background. *Nephrol Dial Transplant* 25: 1059–1066, 2010
 32. Raggi C, Luciani A, Nevo N, Antignac C, Terryn S, Devuyst O: De-differentiation and aberrations of the endolysosomal compartment characterize the early stage of nephropathic cystinosis. *Hum Mol Genet* 23: 2266–2278, 2014
 33. Ivanova EA, De Leo MG, Van Den Heuvel L, Pastore A, Dijkman H, De Matteis MA, et al.: Endo-lysosomal dysfunction in human proximal tubular epithelial cells deficient for lysosomal cystine transporter cystinosis. *PLoS One* 10: e0120998, 2015
 34. Festa BP, Chen Z, Berquez M, Debaix H, Tokonami N, Prange JA, et al.: Impaired autophagy bridges lysosomal storage disease and epithelial dysfunction in the kidney. *Nat Commun* 9: 161, 2018
 35. Sansanwal P, Yen B, Gahl WA, Ma Y, Ying L, Wong LJ, et al.: Mitochondrial autophagy promotes cellular injury in nephropathic cystinosis. *J Am Soc Nephrol* 21: 272–283, 2010
 36. Napolitano G, Johnson JL, He J, Rocca CJ, Monfregola J, Pestonjamas P, et al.: Impairment of chaperone-mediated autophagy leads to selective lysosomal degradation defects in the lysosomal storage disease cystinosis. *EMBO Mol Med* 7: 158–174, 2015
 37. Andrzejewska Z, Nevo N, Thomas L, Chhuon C, Bailleux A, Chauvet V, et al.: Cystinosin is a component of the vacuolar H⁺-ATPase-regulator-rag complex controlling mammalian target of rapamycin complex 1 signaling. *J Am Soc Nephrol* 27: 1678–1688, 2016
 38. Lobry T, Miller R, Nevo N, Rocca CJ, Zhang J, Catz SD, et al.: Interaction between galectin-3 and cystinosin uncovers a pathogenic role of inflammation in kidney involvement of cystinosis. *Kidney Int* 96: 350–362, 2019
 39. Shan J, Jokela T, Peltoketo H, Vainio S: Generation of an allele to inactivate Wnt4 gene function conditionally in the mouse. *Genesis* 47: 782–788, 2009
 40. Leheste JR, Melsen F, Wellner M, Jansen P, Schlichting U, Renner-Müller I, et al.: Hypocalcemia and osteopathy in mice with kidney-specific megalin gene defect. *FASEB J* 17: 247–249, 2003
 41. Chabli A, Aupetit J, Raehm M, Ricquier D, Chadefaux-Vekemans B: Measurement of cystine in granulocytes using liquid chromatography-tandem mass spectrometry. *Clin Biochem* 40: 692–698, 2007
 42. García-Villoria J, Hernández-Pérez JM, Arias A, Ribes A: Improvement of the cystine measurement in granulocytes by liquid chromatography-tandem mass spectrometry. *Clin Biochem* 46: 271–274, 2013
 43. Jouret F, Bernard A, Hermans C, Dom G, Terryn S, Leal T, et al.: Cystic fibrosis is associated with a defect in apical receptor-mediated endocytosis in mouse and human kidney. *J Am Soc Nephrol* 18: 707–718, 2007
 44. Mori K, Lee HT, Rapoport D, Drexler IR, Foster K, Yang J, et al.: Endocytic delivery of lipocalin-siderophore-iron complex rescues the kidney from ischemia-reperfusion injury. *J Clin Invest* 115: 610–621, 2005
 45. Jobst-Schwan T, Knaup KX, Nielsen R, Hackenbeck T, Buettner-Herold M, Lechler P, et al.: Renal uptake of the antiapoptotic protein survivin is mediated by megalin at the apical membrane of the proximal tubule. *Am J Physiol Renal Physiol* 305: F734–F744, 2013
 46. Dachy A, Paquot F, Debray G, Bovy C, Christensen EI, Collard L, et al.: In-depth phenotyping of a Donnai-Barrow patient helps clarify proximal tubule dysfunction. *Pediatr Nephrol* 30: 1027–1031, 2015
 47. Nielsen R, Christensen EI, Birn H: Megalin and cubilin in proximal tubule protein reabsorption: From experimental models to human disease. *Kidney Int* 89: 58–67, 2016
 48. Theilig F, Kriz W, Jerichow T, Schrade P, Hähnel B, Willnow T, et al.: Abrogation of protein uptake through megalin-deficient proximal tubules does not safeguard against tubulointerstitial injury. *J Am Soc Nephrol* 18: 1824–1834, 2007
 49. Weyer K, Andersen PK, Schmidt K, Mollet G, Antignac C, Birn H, et al.: Abolishment of proximal tubule albumin endocytosis does not affect plasma albumin during nephrotic syndrome in mice. *Kidney Int* 93: 335–342, 2018
 50. Christensen EI, Maunsbach AB: Effects of dextran on lysosomal ultrastructure and protein digestion in renal proximal tubule. *Kidney Int* 16: 301–311, 1979
 51. Schiller A, Taugner R: The renal handling of low molecular weight polyvinylpyrrolidone and inulin in rats. In: *Functional Ultrastructure of the Kidney*, edited by Maunsbach AB, Steen Olsen T, Christensen EI, London, Academic Press, 1980, pp 315–326
 52. Barone R, Van Der Smissen P, Devuyst O, Beaujean V, Pauwels S, Courtoy PJ, et al.: Endocytosis of the somatostatin analogue, octreotide, by the proximal tubule-derived opossum kidney (OK) cell line. *Kidney Int* 67: 969–976, 2005
 53. Behr TM, Sharkey RM, Sgouros G, Blumenthal RD, Dunn RM, Kolbert K, et al.: Overcoming the nephrotoxicity of radiometal-labeled immunoconjugates: Improved cancer therapy administered to a nude mouse model in relation to the internal radiation dosimetry. *Cancer* 80 [Suppl]: 2591–2610, 1997
 54. McNeal CJ, Meiningner CJ, Reddy D, Wilborn CD, Wu G: Safety and effectiveness of arginine in adults. *J Nutr* 146: 2587S–2593S, 2016
 55. Molema F, Gleich F, Burgard P, van der Ploeg AT, Summar ML, Chapman KA, et al.: Additional individual contributors from E-IMD: Evaluation of dietary treatment and amino acid supplementation in organic acidurias and urea-cycle disorders: On the basis of information from a European multicenter registry [published online ahead of print February 8, 2019]. *J Inherit Metab Dis* doi: 10.1002/jimd.12066
 56. Elpeleg N, Korman SH: Sustained oral lysine supplementation in ornithine delta-aminotransferase deficiency. *J Inherit Metab Dis* 24: 423–424, 2001
 57. Morris SM Jr.: Arginine metabolism revisited. *J Nutr* 146: 2579S–2586S, 2016
 58. Wolfson RL, Sabatini DM: The dawn of the age of amino acid sensors for the mTORC1 pathway. *Cell Metab* 26: 301–309, 2017
 59. Gahl WA, Balog JZ, Kleta R: Nephropathic cystinosis in adults: Natural history and effects of oral cysteamine therapy. *Ann Intern Med* 147: 242–250, 2007
 60. Cherqui S, Sevin C, Hamard G, Kalatzis V, Sich M, Pequignot MO, et al.: Intralysosomal cystine accumulation in mice lacking cystinosin, the protein defective in cystinosis. *Mol Cell Biol* 22: 7622–7632, 2002

AFFILIATIONS

¹Cell Biology Unit, de Duve Institute and Université Catholique de Louvain, Brussels, Belgium; ²Biochemical Genetics, Academic Hospital Saint-Luc, Brussels, Belgium; ³Laboratory of Hereditary Kidney Diseases, Institut National de la Santé et de la Recherche Médicale (INSERM) U1163, Imagine Institute, Paris Descartes University, Paris, France; ⁴Faculty of Biochemistry and Molecular Medicine, Laboratory of Developmental Biology, Oulu Center for Cell-Matrix Research, Biocenter Oulu, University of Oulu, Oulu, Finland; ⁵Department of Biomedicine, Aarhus University, Aarhus, Denmark; and ⁶Groupe Interdisciplinaire de Génoprotéomique Appliquée (GIGA), Cardiovascular Sciences, University of Liège, Liège, Belgium